Assessment of canal bank stability with vegetation root reinforcement

Kamath, Abhijith; van Bergen, Karine; Ravenshorst, Geert; van de Kuilen, Jan-Willem

DOI
10.1016/j.ecoleng.2025.107623

Publication date
2025

Document Version
Final published version

Published in
Ecological Engineering

Citation (APA)
Kamath, A., van Bergen, K., Ravenshorst, G., & van de Kuilen, J.-W. (2025). Assessment of canal bank stability with vegetation root reinforcement. *Ecological Engineering*, *217*, Article 107623. https://doi.org/10.1016/j.ecoleng.2025.107623

Ecological Engineering 217 (2025) 107623

Contents lists available at ScienceDirect

Ecological Engineering

journal homepage: www.elsevier.com/locate/ecoleng

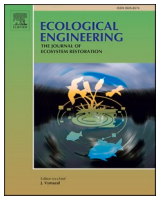

Assessment of canal bank stability with vegetation root reinforcement

Abhijith Kamath [a,*], Karine van Bergen [a], Geert Ravenshorst [a], Jan-willem van de Kuilen [a,b]

[a] Department of Engineering Structures, Biobased Structures and Materials Group, Delft University of Technology, Stevinweg 1, 2628 CN Delft, the Netherlands
[b] Wood Technology, Technical University of Munich, Winzererstrasse 45, 80797 Munich, Germany

ARTICLE INFO

Keywords:
Stream bank protection
Root reinforcement
Nature based solutions
Root area ratio

ABSTRACT

There is an increasing need for using nature based solutions in protecting canal and stream embankments in the Netherlands and delta areas in general. Vegetation provides additional reinforcement and forms an integral part of many nature-based solutions. However, quantifying this reinforcement in-situ is challenging. This study aims to quantify the root reinforcement of three species prevalent along canal embankments – *Salix fragilis* L. (SF), *Salix purpurea* L. (SP), and *Crataegus laevigata* DC. (CL) – using the corkscrew extraction technique. Furthermore, canal bank stability was analyzed under different bank conditions regarding protection (unprotected, protected by vegetation), bank geometry, and hydraulic conditions.

Quantity of roots and Root Area Ratio (RAR) generally decreased with depth for all species. While root breakage was observed in most samples, all species exhibited increased ductility with higher root densities, except for CL at two depths. SF showed higher root reinforcement at shallower depths ($\leq$ 250 mm), while SP demonstrated greater reinforcement at deeper depths. Results demonstrate that the corkscrew extraction technique is a quick and minimally invasive method for measuring root reinforcement in riparian environments.

Bank stability simulations revealed that vegetation significantly increases the stability of canal banks. Notably, when considering measured root reinforcement, the factor of safety improved dramatically from 1.08 to 2.46, even under analyzed worst case conditions. However, the analysis suggests a limiting root reinforcement beyond which further increases in root reinforcement have minimal impact on stability. Monitoring using the corkscrew apparatus and future design approaches could aim to achieve this minimum reinforcement.

1. Introduction

Protecting canal and riverbanks is important for economic, cultural, environmental, and navigational reasons. Bioengineered bank protection techniques are increasingly favored over methods like riprap because they can regulate riparian ecosystem functions and services. Furthermore, using natural materials offers a potential reduction in carbon emissions (Symmank et al., 2020).

Bioengineered constructions generally consist of an inert component (in this case, wood) and a living component (vegetation). These systems are based on the principle that while the inert component, such as locally sourced wood, may decay, the living component—vegetation—will develop roots over time, providing support to the slope (Tardio and Mickovski, 2023). The inert element's purpose is to protect the slope until the vegetation's root system is sufficiently established to bear the load. The effectiveness of bioengineered structures depends on the progressive transfer of load from the inert to the living elements over time (Tardío and Mickovski, 2016). Therefore, quantifying and monitoring the vegetation's capacity to support the slope is crucial for the successful application of bioengineered bank protection.

Vegetation contributes to slope stability by mechanically and hydrologically reinforcing the soil (Fan and Su, 2008; Giadrossich et al., 2017; Capobianco et al., 2021). Accurately assessing root reinforcement is challenging due to variations in root architecture and tensile strength both between and within species (Fan and Chen, 2010; Boldrin et al., 2017). Nevertheless, numerous studies have quantified root reinforcement experimentally, including using conventional techniques such as

Abbreviations: SF, *Salix fragilis* L.; SP, *Salix purpurea* L.; CL, *Crataegus laevigata* DC.; RAR, Root Area Ratio; S1, Site 1; S2, Site 2; P1, Plot 1; P2, Plot 2; FS, Factor of Safety; n_i, Number of roots with diameter i; $A_{r,i}$, Cross sectional area of root; F_n, Normalized peak force; J_n, Normalized peak energy; $F_{r,peak}$,, Peak force of the samples (N); $F_{ls,peak}$, Peak force of least rooted samples (N); J_{ls}, Peak energy of least rooted soil (Nmm); J_r, Peak energy of the sample(Nmm); BSTEM, Bank Stability and Toe Erosion Model.

* Corresponding author.
E-mail address: A.C.Kamath@tudelft.nl (A. Kamath).

https://doi.org/10.1016/j.ecoleng.2025.107623
Received 31 May 2024; Received in revised form 18 March 2025; Accepted 25 March 2025
Available online 16 April 2025

direct shear tests. These tests have been conducted in situ under field conditions (Docker and Hubble, 2008; Fan and Tsai, 2016) or in large direct shear boxes where vegetation is cultivated under controlled conditions (Ghestem et al., 2014; Yildiz et al., 2018). While the latter approach offers the advantage of repeatable testing under similar conditions, the former allows for direct measurement and real-time monitoring of root reinforcement. Although less common, triaxial tests (Zhang et al., 2010) and vane shear tests (Krzeminska et al., 2019) have also been used to directly quantify the additional reinforcement provided by roots.

Remote landscapes, such as riparian areas, present several challenges for conducting shear tests. Firstly, transporting and setting up shear equipment, such as a direct shear apparatus, is cumbersome. Secondly, destructive testing methods are unsuitable for continuous monitoring of root reinforcement. Lastly, as previously mentioned, the natural variability in root distribution necessitates a large number of tests over time, which can be labor-intensive.

Meijer et al. (2016) and Meijer et al. (2018) developed a corkscrew apparatus for estimating root reinforcement, claiming it to be quick and easy to use, particularly in mountainous terrains. Liang et al. (2020) suggested using testing methods such as the corkscrew, where a hand-held device could be used for rapid testing, rather than relying on a few expensive and detailed methods like direct shear. To the best of the authors' knowledge, corkscrew extraction experiments have not yet been employed to determine reinforcement due to the presence of roots along streambanks. The apparatus developed by Meijer et al. (2016) and Meijer et al. (2018) is used in this study to experimentally determine root reinforcement and to assess the applicability of the method to streambank protection research.

The factor of safety (FS) of a canal bank can be estimated as the ratio of resisting forces to driving forces. Hydrological loads, such as high-intensity rainfall and melting snow, or human activities, such as tractor loads, can act as triggering driving forces toward embankment failure (Krzeminska et al., 2019). The additional strength provided to the soil by vegetation, along with the inherent soil strength, resists these driving forces. The Bank Stability and Toe Erosion Model (BSTEM), developed by the National Sedimentation Laboratory in Oxford, USA, can be used to estimate streambank stability (Simon et al., 2000; Pollen-Bankhead and Simon, 2009; Midgley et al., 2012; Krzeminska et al., 2019). Several studies have used and validated the BSTEM model to evaluate bank stability (Klavon et al., 2017; Rasouli et al., 2020; LeRoy et al., 2024).

This study focuses on three common species found along canal embankments in the Netherlands: *Salix fragilis* L. (SF), *Salix purpurea* L. (SP), and *Crataegus laevigata* DC. (CL). The selected species are native and were selected for their prevalence in riparian ecosystems within the Dutch landscape. Particularly *Salix* species are well-adapted to riparian environments. Furthermore, these species are readily available and commonly used in ecological engineering projects within the Netherlands.

The aim of this study is to quantify the contribution of the above three riparian vegetation species to the stability of canal banks using a combination of field measurements and bank stability modelling. The research also aims to provide valuable insights into the effectiveness of these native species in enhancing bank stability and to evaluate the applicability of the corkscrew extraction method for assessing root reinforcement in riparian environments.

2. Material and methods

2.1. Location and profile

The experimental tests were conducted at two locations. Site number 1 (S1) was located at Hortus Botanicus of TU Delft (52.008390, 4.369684) along an unprotected stream with a width of about 3 m. Site number 2 (S2) was located at the bank of a sheet pile protected canal at Middenmeer, Province of North Holland (52°48′07.8"N 4°59′50.8″E).

Soil was collected at both sites, oven-dried at 105 °C, and subjected to dry sieving. The soil type at S1 and at S2 was determined to be poorly graded sand according to USCS classification. Bulk density at site 1 was 18 kN/m^3 and at site 2 was 16 kN/m^3.

Vegetation.

Two plots with two different species of vegetation commonly known as 'Willow' were tested at S1. First plot (S1P1) had one *SF* plant (commonly known as Crack willow) and second plot (S1P2) had one SP plant (commonly known as Purple willow). SF was located around 0.75 m distance from edge of the bank and the SP tree was located 1 m from the edge of the bank (Fig. 1). SF had a diameter at breast height (DBH) of 0.6 m and SP had a DBH of 1.1 m. There were randomly located grass patches at both the plots. At S2, testing was conducted at a plot (S2P1) that had only two plants of CL (commonly known as Midland hawthorn) in the vicinity.

2.2. Corkscrew equipment

The corkscrew test setup developed by Meijer et al. (2016) and Meijer et al. (2018) was adopted for determining the strength of root-reinforced soil. The setup consists of a corkscrew which is a commercially available garden tool used to remove weeds. Corkscrew deweeder manufactured by DeWit Kornhorn BV was used in this study. The corkscrew was connected through a loadcell of 5 kN to a cable. The cable was connected to a mechanical winch which was placed on a tripod. A draw wire displacement sensor (model WPS250-MK30-P10, Micro-Epsilon, Ortenburg, Germany) was also placed to measure displacement of the corkscrew. A datalogger box that records load and displacement at a frequency of 2 Hz was also fixed on top of the tripod, making the full setup easy to transport (Fig. 2).

The testing procedure involves manually rotating the corkscrew to the desired depth. The tripod with the measuring sensors and winch was placed vertically on top of the corkscrew. The draw-wire sensor is subsequently attached to the load cell, ensuring that both draw wire and steel wires are parallel in order to avoid any non-linearity-related corrections in displacement. The tests were conducted at a withdrawal speed of 2 mm/s which corresponds to displacement rates of slow landslides (Meijer et al., 2016).

2.3. Data collection

Soil moisture content for each depth was determined. A small sample of the core was placed in the oven at 105 °C for 24 h for moisture content measurements. Soil water potential was measured at depths of 0.3 m and 0.5 m at site S1, and at depths of 0.25 m and 0.5 m at site S2, throughout the testing period using plug-in tensiometers (Stelzner®, Pronova.de). The soil was saturated at both locations during the period of testing.

After each core was extracted, diameters of roots protruding out from the sample were measured using a vernier caliper. All the cores collected were wrapped in cling film tightly and stored in air-tight box. The cores were transported to the laboratory and weighed with a scale of precision 0.01 g. The extracted soil cores were washed over a 2 mm sieve to collect all root material, as illustrated in Fig. 3. The holes formed by cores in superficial layers were examined for any broken roots that had been pulled out. If such roots were found, they were cut and included with the roots obtained from rest of the core. When biomass had to be measured, the roots were oven-dried at 40^{0}C until no rate of change of biomass was measured.

The Root Area Ratio (RAR) was determined as:

$$RAR\ (\%) = \frac{\sum_i n_i A_{r,i}}{A} * 100 \quad (1)$$

where A is the cross-sectional area of the shear plane, n_i is the number of roots with diameter i intersecting the shear plane and $A_{r,i}$ is the cross

Fig. 1. Corkscrew extraction measurement locations: a) *Salix fragilis* L. b) *Salix purpurea* L. c) *Crataegus laevigata* DC.

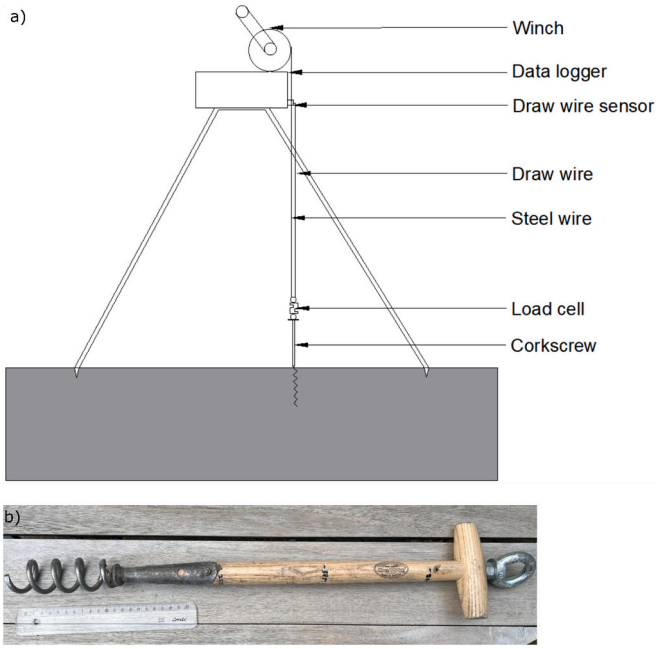

Fig. 2. Experimental setup a) Schematic corkscrew extraction measurement setup (Adapted from Meijer et al., 2018) b) Corkscrew device.

sectional area of a single root with diameter i.

The energy required to extract a volume of rooted soil from the ground, denoted as J (Eq. (2)) was determined by calculating the total area beneath the force (F)-displacement curve.

$$J = \int_{u0}^{u} F(u)du \tag{2}$$

$u_0 = 0$ mm and u denotes the displacement at the end of test.

In order to account for the additional force provided by the roots alone, the peak force and energy of the rooted-soil composite is normalized (Eq. (3), Eq. (4)) with the peak force and energy of least rooted soil at that depth as:

$$F_n = \frac{F_{r,peak}}{F_{ls,peak}} \tag{3}$$

$$J_n = \frac{J_r}{J_{ls}} \tag{4}$$

F_n is the normalized peak force, J_n is the normalized energy, J_r is the energy of the sample (Nmm), $F_{r,peak}$, represents the peak force of the samples (N) and $F_{ls,peak}$, represents the peak force of least rooted samples (N), J_{ls} represents the energy of least rooted soil (Nmm).

The tests at S1 were conducted during October 2022 and March 2023 for P1 and P2 respectively, see Table 1**.** Tests at S2 were conducted in March 2023. To take the spatial variation of the root reinforcement into account, tests at P1 were conducted at distances between 200 mm and 600 mm from SF. At P2, tests were conducted at a distance varying between 200 mm and 1000 mm from the SP (Fig. 4**).**

2.4. Modelling

The BSTEM model, developed by the USDA-ARS National Sedimentation Laboratory in Oxford, USA, is a physically based model used for analyzing multi-layered streambanks (Simon et al., 2000; Simon et al., 2009; Pollen-Bankhead and Simon, 2009; Simon et al., 2011). BSTEM accepts input parameters such as bank geometry (bank height, slope angle, layer thickness), soil properties (cohesion, internal friction angle, unit weight, and hydraulic conductivity for each layer), hydraulic conditions (groundwater table depth and stream stage). BSTEM uses limit equilibrium principles to assess bank stability by comparing driving forces against resisting forces. The shear strength of saturated soil is determined using the Mohr-Coulomb failure criterion. BSTEM allows for the consideration of five distinct layers and incorporates the influence of pore water pressures on both the saturated and unsaturated portions of the failure surface, as well as the confining pressure from streamflow. BSTEM assumes a horizontal water table within the bank and calculates pore pressures for each layer under hydrostatic conditions based on the provided groundwater table depth. BSTEM can model shear-type failures that occur when the driving force (stress) exceeds the resisting forces.

BSTEM uses an inherent algorithm, iterating through various failure scenarios (including shear emergence elevations and shear surface angles) to identify the configuration yielding the minimum FS. Bank stability is confirmed when the calculated FS exceeds 1.3, while banks with an FS between 1.0 and 1.3 are considered “conditionally stable,” indicating stability but with a limited buffer for uncertain or fluctuating data. Slopes with an FS below 1.0 are classified as “unstable” (Simon et al., 2000).

Fig. 3. Collection and processing of corkscrew extraction samples. a) Root diameter measurement using calipers. b) Root collection from the extracted soil sample. c) Water content measurements and drying of roots in an oven. d) Holes formed in the embankment after corkscrew extraction.

Table 1
Details of corkscrew testing locations and time of testing.

Testing location	Month-year	Location	Spatial distance of testing
S1P1	October 2022	Hortus Botanicus, Delft	200–600 mm
S1P2	March 2023	Hortus Botanicus, Delft	200–1000 mm
S2P1	March 2023	Kolhornerweg, Middenmeer	500 mm

BSTEM considers the mechanical role of vegetation in bank stability by modifying soil strength parameters using the RipRoot model (Pollen and Simon, 2005; Pollen, 2007) to incorporate root reinforcement. RipRoot is a fiber bundle-based model that simulates root reinforcement by representing the root system as a network of interconnected fibers with global load-sharing characteristics. It can simulate both root breakage and pullout. It allows for the consideration of key root characteristics, such as root diameter and tensile strength, that influence the reinforcement provided by the vegetation. Thus, RipRoot can simulate various root failure mechanisms under increasing shear stress. This

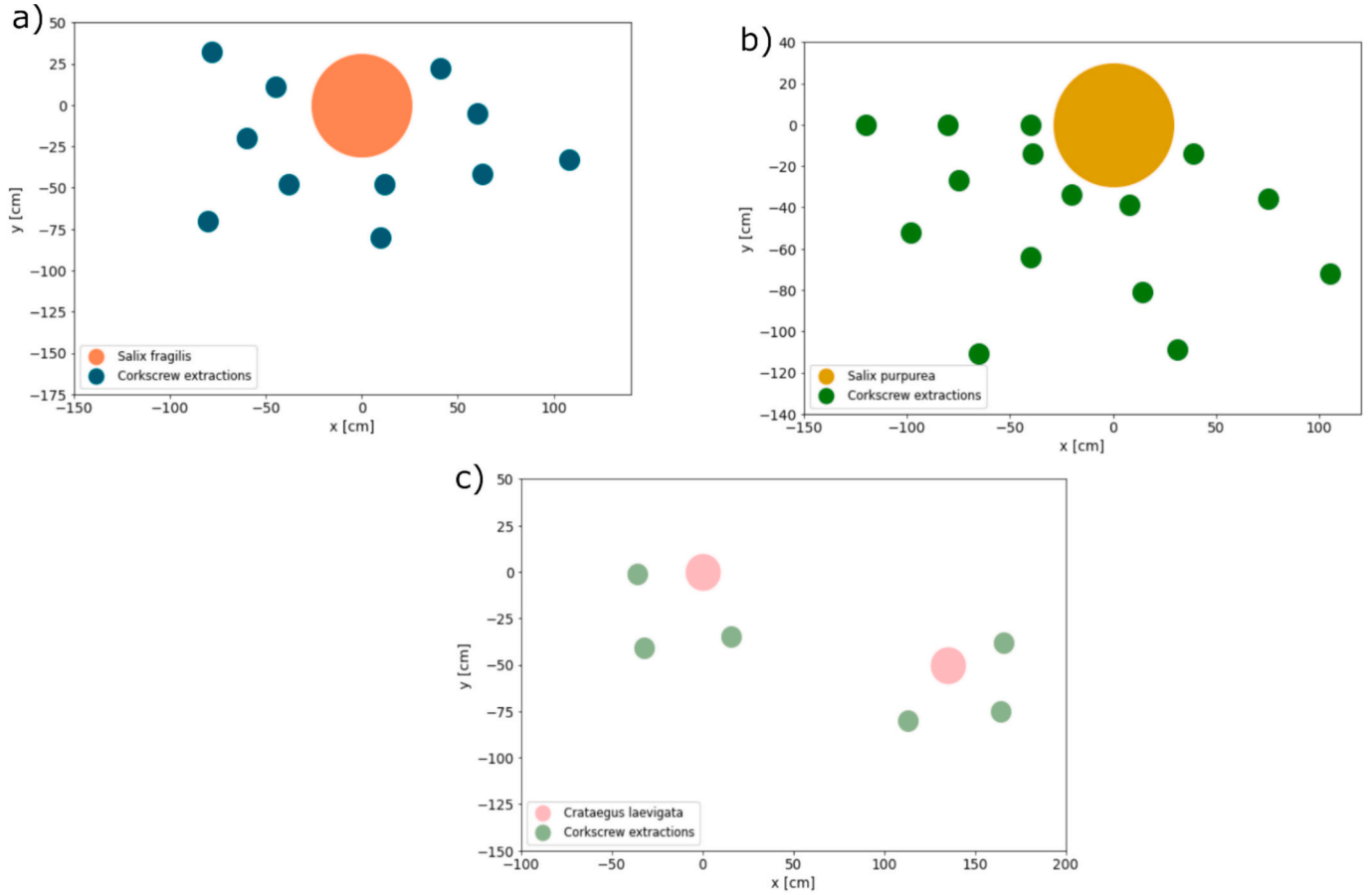

Fig. 4. Plan view of spatial distribution of corkscrew extraction experiments with respect to the vegetation a) *Salix fragilis* L. b) *Salix purpurea* L. c) *Crataegus laevigata* DC.

mechanistic approach provides a more realistic representation of root behavior under loading compared to simpler empirical models. The background and detailed mathematical formulations for BSTEM and the RipRoot model can be found in Simon et al. (2000), Pollen (2007), and Ursic and Langendoen (2021).

The BSTEM model allows the user to select species, corresponding diameter-tensile strength relationships, and growth curves measured by a USDA-ARS-NSL scientist. Alternatively, the user can input their own data for all of the above and also the percentage of the study reach composed of the selected species.

2.5. Modelling strategy

Three different groups of input parameters were created for the BSTEM model. The difference between each group depended on how vegetation reinforcement was determined.

(i) The first group (G1) of input parameters was based on the RipRoot fiber bundle model Pollen and Simon (2005), which is integrated within BSTEM. To represent *Phragmites australis* L. (PA), a grass species, "Canarygrass, Reed+" was chosen with a plant age of 5 years and 100 % assemblage. For *SF.*, "Willow, Geyer's" was chosen with an age of 10 years and 100 % contribution to the assemblage. *SP* was represented using the "Willow, Black" option in BSTEM, with an age of 10 years and 100 % contribution to the assemblage.

(ii) The second group (G2) was based on a representative increase in shear strength obtained from the corkscrew experimental results. For each species and depth, the minimum peak strength (representing the least rooted/bare soil) measured from the corkscrew experiments was subtracted from the average peak strength (average strength of rooted soil). Furthermore, the average of the resulting strength increases was used as input for the BSTEM model, as it would represent an average increase in strength due to the presence of roots.

(iii) The third group (G3) was based on a conservative expert estimate that considered the corkscrew experimental results for each species, strength variations from the RipRoot fiber bundle model, and relevant literature. Similar expert estimates were used by Krzeminska et al. (2019) in their BSTEM model.

2.6. Modelling scenarios

The aim of this modelling exercise was to estimate the FS of the bank at S1 under different scenarios. In the first step, the current stability state of the S1 bank is investigated with SF, SP, PA.

The experimental results for PA reed reported in Kamath et al. (2023), for the same site but on the other bank of the stream, are adopted here. The bank geometry modelled was based on S1 (Fig. 5). A bank with a height of 1.5 m, a bank angle of 40°, a bank toe length of 0.5 m, and a bank toe angle of 90° is modelled. A flow water elevation in the stream of 0.25 m is input.

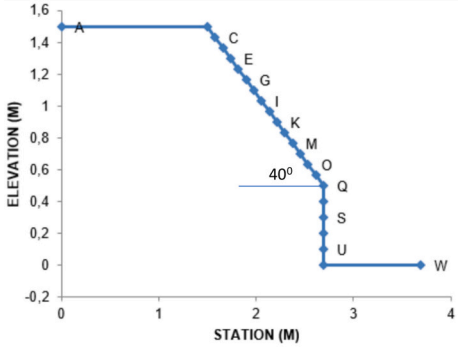

Fig. 5. Input geometry of the bank used in BSTEM model.

In addition, the following scenarios are also modelled:

(i) Water table rises to surface
(ii) Bank angle increases from 40^0 to 55^0
(iii) Flow water elevation in the stream changes to 0.75 m and 0 m.

In total 8 cases were analyzed (Table 2).

3. Results

A total of 28, 32, and 19 successful corkscrew extraction experiments were conducted at Site 1, plot 1 (SF); Site 1, plot 2 (SP); and Site 2, plot 1 (CL), respectively. The corkscrew experiments extended from 0 to 375 mm for the plot with SF and up to 500 mm for the other two plots. Minimum RAR values of 0.003 %, 0.001 %, and 0.01 % were obtained for SF, SP, and CL, respectively. Similarly, maximum RAR values of 0.772 %, 0.873 %, and 0.238 % were obtained for SF, SP, and CL, respectively. The maximum RAR for SF and CL was obtained in the superficial layer (0–125 mm), while the maximum RAR for SP was obtained in a deeper layer (0–375 mm). A moisture content greater than 34 % was recorded for all plots at all depths.

3.1. Site 1, plot 1-Salix fragilis L

Maximum root biomass and RAR were found in cores taken from a 0–125 mm depth. Sixty-two percent of the root biomass and approximately 65 % of the RAR were concentrated at this shallowest depth (0–125 mm) (Fig. 6). Comparison of the least rooted and most rooted soil shows that the peak force of the soil with the highest quantity of roots was greater than that of the least rooted soil at all depths. Similarly, the displacement at peak force was also less for the least rooted soil at depths of 0–125 mm and 125–250 mm. However, the displacement at peak force at a depth of 250–375 mm was in a similar range (10–28 mm) for all tests.

In general, two distinct force-displacement responses were observed in the tests. Type 1 shows a rapid increase in force over a short distance followed by a gradual decrease over a longer displacement. Type 2 shows a rapid increase in force over a short distance followed by a gradual increase in force instead of a decrease, possibly due to root engagement (Fig. 7).

Another feature observed in the force-displacement graphs is the sudden drop in force (Fig. 8). This sudden drop is attributed to root breakage. Post-test analysis identified broken roots in those tests where sudden drops were observed. The characteristics mentioned above

Table 2
List of cases analyzed in BSTEM model.

Cases	Water table (WT) (m)	Flow water elevation (WE) (m)	Bank angle (BA) (^{0})
Case-1	0	0.25	40
Case-2	0.25	0.25	40
Case-3	0	0	40
Case-4	0.25	0	40
Case-5	0	0.75	40
Case-6	0.25	0.75	40
Case-7	0.25	0.25	55
Case-8	0	0.25	55

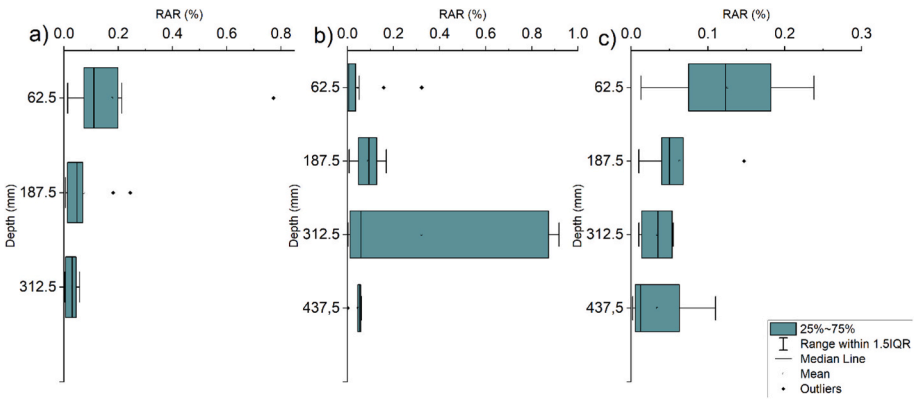

Fig. 6. Root area ratio variation with depth a) *Salix fragilis* L. b) *Salix purpurea* L. c) *Crataegus laevigata* DC.

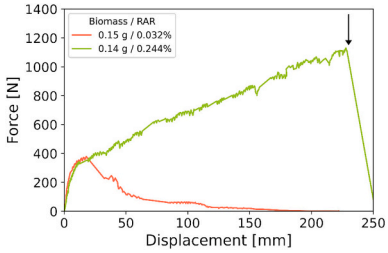

Fig. 7. Example force-displacement curves observed for Type 1 (red line) and Type 2 (green line) in corkscrew experiments from *Salix fragilis* L. Type 1 has a lower biomass (0.15 g) and a lower root area ratio (RAR, 0.032 %), while Type 2 has a similar biomass (0.14 g) and a higher RAR (0.244 %). The arrow indicates a potential root breakage. (For interpretation of the references to colour in this figure legend, the reader is referred to the web version of this article.)

indicate that rooted samples exhibit robust ductile behavior when compared with non-rooted samples.

Regardless of depth, the samples with the highest and lowest dry biomass do not correspond to those with the highest and lowest RAR, respectively. For example, at a depth of 0–125 mm, test number 1 has the lowest RAR (Supplementary Material S1) but not the lowest root biomass. It is also interesting to note that this test exhibits Type 1 behavior. Tests 5 (1.77 g) and 7 (0.4 g) at a depth of 0–125 mm exhibit similar Type 2 behavior but have significantly different root biomass (see Supplementary Material S1). Tests 8 and 9 at a depth of 125–250 mm have similar root biomass but different force-displacement behavior. Comparing tests 1 and 11 at a depth of 0–125 mm, test 1 exhibits Type 1 behavior, while test 11 exhibits Type 2 behavior. However, the root biomass of test 1 was higher (0.20 g) than that of test 11 (0.12 g). This anomaly in force-displacement behavior, when compared with root biomass, disappears when RAR is considered.

Tests 5 and 7 at a depth of 0–125 mm show Type 1 curves and have similar RAR values. Tests 8 and 9 at a depth of 125–250 mm have different force-displacement curves, and their RAR values are significantly different. Test 1, at a depth of 0–125 mm, has an RAR value approximately ten times lower than that of test 11 at the same depth, which is consistent with their soil behavior. The disparities observed in the comparison between soil behavior and root biomass indicate that root biomass may not be a precise indicator of root reinforcement. Conversely, when comparing the RAR of the samples, the mentioned variations and anomalies do not persist. This suggests that root biomass may not effectively predict the behavior of rooted soil in corkscrew experiments, while RAR appears to offer a more insightful explanation for the ductile behavior of rooted soils. Considering all samples together and excluding potential outliers, a moderate positive correlation was observed between normalized peak force and RAR ($R^2 = 0.65$) and between normalized energy and RAR ($R^2 = 0.62$) (see Fig. 11).

3.2. Site 1, plot 2-Salix purpurea L

A significant decrease in RAR with depth, as observed in S1P1, was not found in this case. A human-induced experimental error occurred when extracted soil fell back into the hole during testing. Therefore, only 15 cores from the first layer (0–125 mm) and six cores from deeper layers (up to 500 mm) were deemed successful; the remaining tests were rejected. Similar to S1P1, Type 1 and Type 2 curves were observed for tests on SP-rooted soils. In tests on samples with higher RAR (Fig. 9), the force dropped to nearly zero with a very sudden drop. This drop could be attributed to root breakage, as broken roots were recovered in all such tests. Another interesting observation was the distinct clicking/rupturing sound heard with each sudden drop. This suggests that, following soil failure, resistance was predominantly provided by the roots. No correlation was found between normalized peak force and RAR, or between the normalized energy required to extract the sample from the soil and RAR.

3.3. Site 2, plot 1-Crataegus laevigata DC

A marked decline in the RAR of CL was observed with increasing depth, with 53 % of the total RAR concentrated in the shallowest layer (0–125 mm). In general, medium-sized roots (0.2 mm < dr < 1.0 mm) were distributed relatively evenly with depth, while medium-thick roots (dr > 1 mm) rapidly decreased with depth, with over 57 % concentrated in the top layer. Very few thin roots (dr < 0.2 mm) were found in the samples.

The sample with an RAR as low as 0.002 % (the lowest of all tests at Site 2, test number 1 at the 375–500 mm level) also exhibited ductile behavior (see Supplementary Material). At a depth of 125–250 mm, test number 6, with a lower RAR (0.01 %), had a higher peak strength than test number 1, with a higher RAR (0.147 %) (Fig. 10). All roots in test number 6 were in the medium size range (0.2 mm < dr < 1.0 mm), whereas the roots in test number 1 consisted of both medium and thick roots. One thick root in test number 1 slipped, and the other roots broke, while all roots in test number 6 broke. A similar observation was made at a depth of 375–500 mm: the sample with the lowest RAR (test 1) had a similar peak resistance to the sample with the highest RAR (test 4). Post-test analysis showed that the roots in test 4 slipped, with breakage observed only at a displacement of 151 mm, while root breakage in test 1 was observed at a displacement of 50 mm. A positive correlation was observed between RAR and normalized peak force, and between RAR and normalized energy after excluding potential outliers (see Fig. 11).

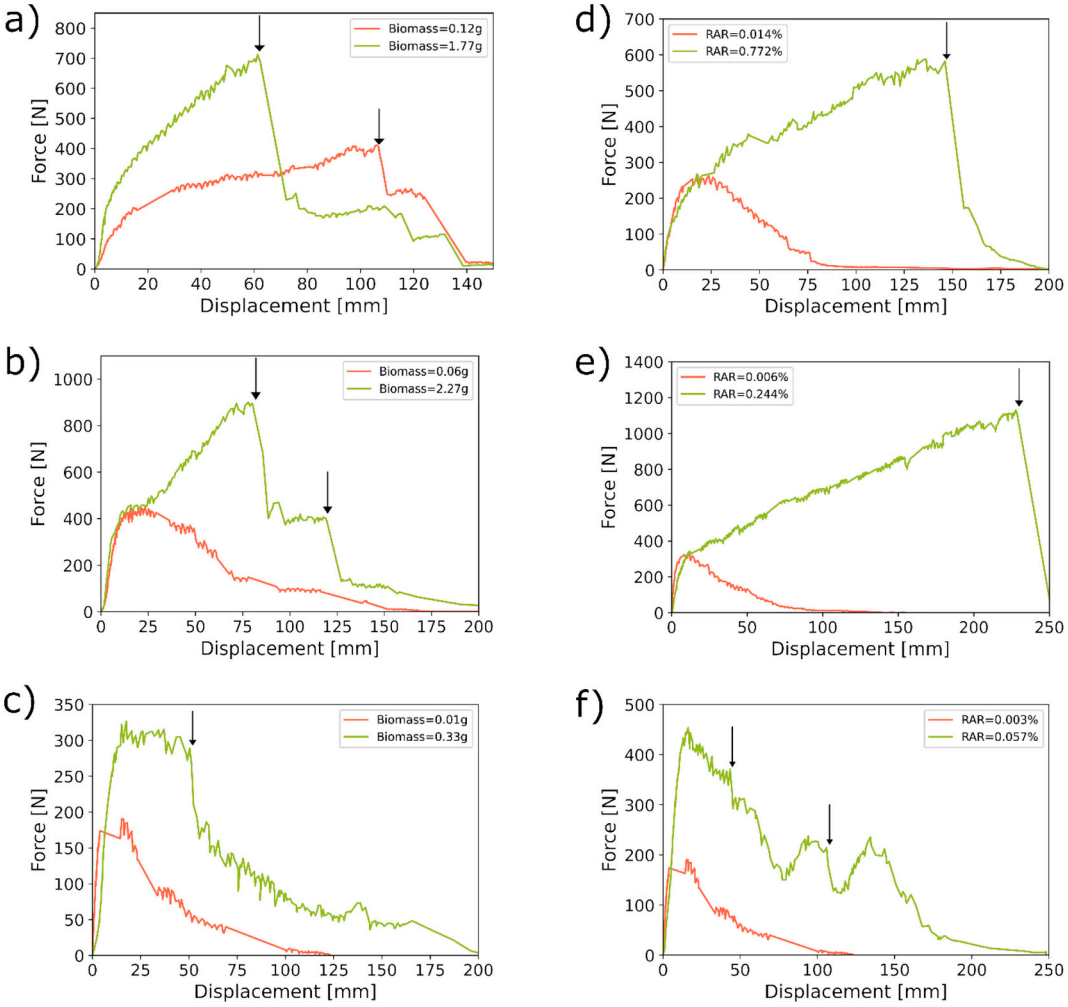

Fig. 8. Example corkscrew extraction force-displacement graphs of soil samples containing roots of *Salix fragilis* L. at depths: a) 0–125 mm, b) 125–250 mm, and c) 250–375 mm. For each depth, graphs are shown for samples with the highest (green line) and lowest (red line) root biomass. In panels d), e), and f), graphs are shown for samples with the highest (green line) and lowest (red line) root area ratio at the same depths. (For interpretation of the references to colour in this figure legend, the reader is referred to the web version of this article.)

3.4. Modelling results

For the modelling, a uniform saturated density of 18 kN/m^3 (obtained at S1) was assigned to all five layers. Bare soil strength parameters, consisting of a friction angle of 42° and cohesion of 1 kPa, were used based on soil strength data from S1 (Supplementary Material S4). The additional cohesion due to vegetation for each group (G1, G2, and G3) was added to the soil cohesion (Table 3). The maximum rooting depth for all plants was limited to 0.75 m due to the high water table and saturated soil conditions observed at the site.

BSTEM automatically calculates the tension crack depth as half the maximum tension crack depth, according to Lohnes and Handy (1968). The BSTEM model was then used for calculation, utilizing its inherent parameter settings. A total of 80 model runs were conducted: 8 for bare soil and 24 each for PA, SF, and SP.

The cohesion estimated in G2, based on the corkscrew test results, was higher for all three vegetation types compared to G1 and G3 (Figs. 12–14). Consequently, the corresponding FS for all three vegetation types in G2 was higher than or equal to that in G1 and G3. In Case 8, the most critical of all cases analyzed (highest bank angle, lowest flow water level, and high water table), the bare soil bank was found to be only conditionally stable, with an FS of 1.08. The FS increased to 2.46 (stable condition) in the presence of PA, SF, and SP, due to the additional cohesion estimated from the experimental results. Comparing Case 7 with Case 8, and Case 1 with Case 2, it can be seen that while the bare soil FS decreased with an increasing water table, the FS was not affected when vegetation reinforcement (G2) was present.

When Cases 1 and 2 are compared under G1 conditions, the FS of PA, bare soil, and SF decreases as the water table rises toward the surface. However, the FS of SP remains constant. Applying the same comparison to the G3 input parameters, the FS of bare soil and PA-rooted soil is influenced by the water table change between Cases 1 and 2, while the FS of SF and SP remains unchanged. This suggests the existence of a critical root-cohesion value above which additional vegetation reinforcement does not influence the FS of a bank under certain conditions. This is further supported by comparing Cases 7 and 8 under G1 and G3 input parameters. A rise in the water table does not influence the FS of the SF and SP-rooted banks under G1 parameters, and it does not influence the SP-rooted bank under G3 parameters.

4. Discussion

4.1. Biomass, root area ratio and peak strength

The observed RAR of 0.003 % to 0.77 % for SF and 0.001 % to 0.91 % for SP is consistent with previously reported RAR values in similar environments, such as lower riverbanks with other species (Abernethy and Rutherfurd, 2001). However, scatter in RAR was observed for all three

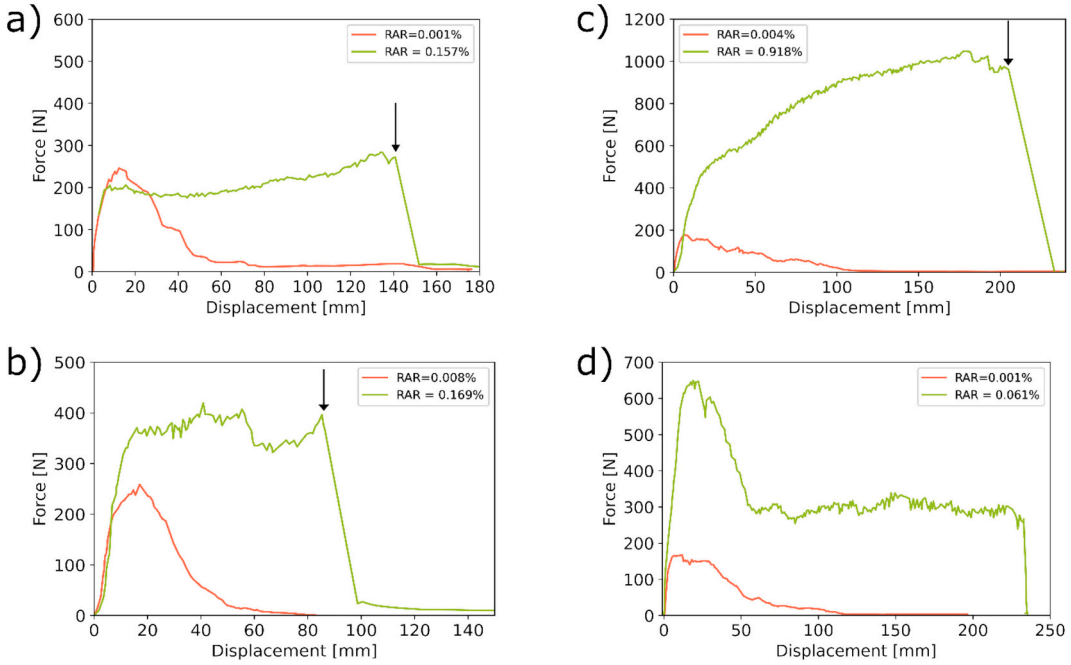

Fig. 9. Example corkscrew extraction force-displacement graphs of soil samples containing roots of *Salix purpurea* L. at depths a) 0–125 mm, b) 125–250 mm, c) 250–375 mm, and d) 375–500 mm. For each depth, the corkscrew tests with the highest (green line) and lowest (red line) root area ratios (RAR) are plotted. Arrows indicate potential root breakages, marked by sudden drops in resistance. (For interpretation of the references to colour in this figure legend, the reader is referred to the web version of this article.)

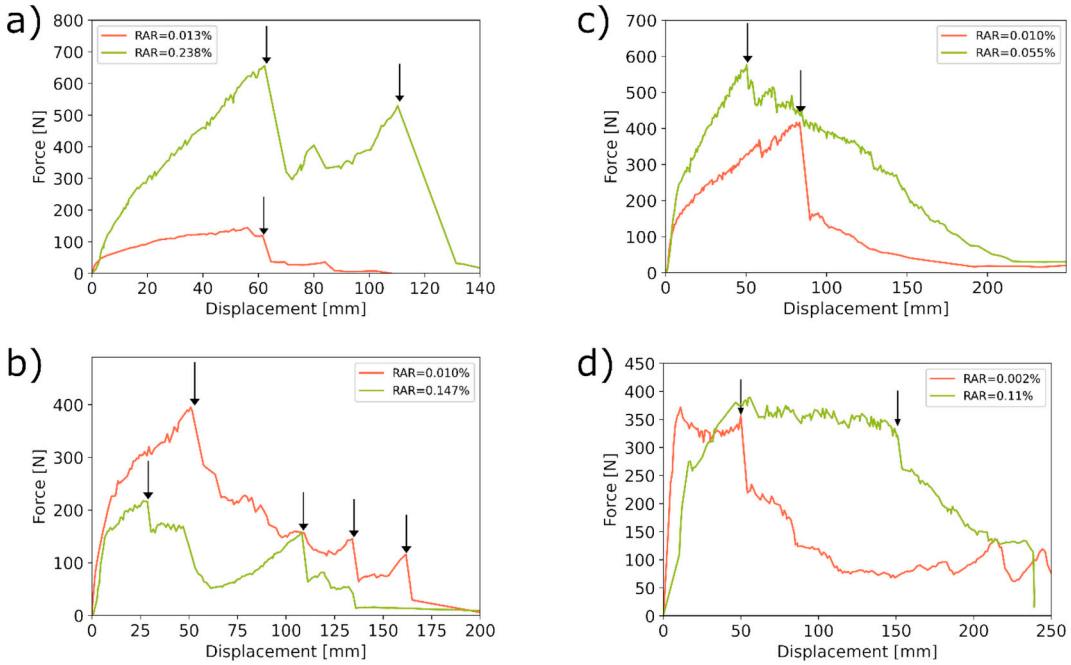

Fig. 10. Force-displacement curves from corkscrew extraction tests on soil samples containing roots of *Crataegus laevigata* DC. at different depths: a) 0–125 mm, b) 125–250 mm, c) 250–375 mm, and d) 375–500 mm. For each depth, the curves represent tests with the highest (green line) and lowest (red line) root area ratios. Arrows indicate potential root breakages, marked by sudden drops in resistance. (For interpretation of the references to colour in this figure legend, the reader is referred to the web version of this article.)

species at every sampling depth of the corkscrew core. Bischetti et al. (2005) also observed high RAR variability related to species, location, and depth in their study of five species at three different locations in Lombardy, Italy. Site 1's close proximity to water suggests that any observed scatter may have been influenced by other stress factors.

Researchers have successfully used root biomass to compare different root reinforcement treatments in direct shear tests (Yildiz et al., 2018) and to analyze strength variation in relation to root biomass in triaxial tests (Alam et al., 2022). However, in the current study, tests on SF-rooted soil and a previous study on *PA*-rooted soil (Kamath et al., 2023) showed a lack of correlation between peak strength, energy, and root biomass. A root contributes to the strength of the root-soil

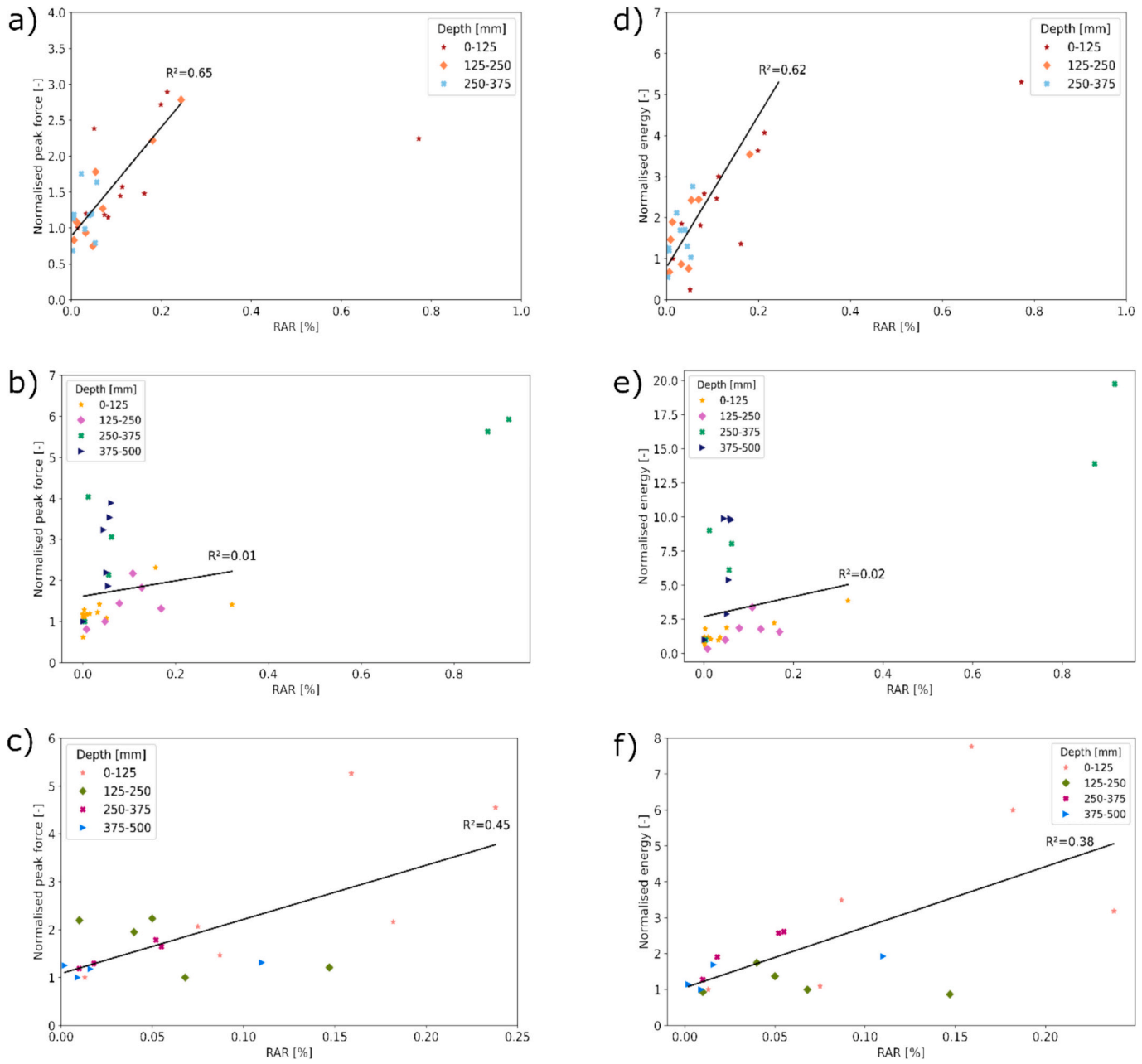

Fig. 11. Relationship between root area ratio (RAR, %) and normalized peak force for (a) *Salix fragilis* L. (SF), (b) *Salix purpurea* L. (SP), and (c) *Crataegus laevigata* DC. (CL), and between RAR (%) and normalized energy for (d) SF, (e) SP, and (f) CL. Data points are differentiated by depth interval: 0–125 mm, 125–250 mm, 250–375 mm, and 375–500 mm (where applicable). Linear trendlines and corresponding R^2 values are shown. Potential outliers were excluded from the regression analysis.

Table 3
Additional root reinforcement input into BSTEM model. PA-*Phragmites Australis* L., SF-*Salix fragilis* L., SP-*Salix purpurea* L.. G1, G2, G3 represents three different groups of root reinforcement.

Layer	Depth	Cohesion (cr)								
		PA			SF			SP		
		G 1	G 2	G 3	G 1	G 2	G 3	G 1	G 2	G 3
	[m]	[kPa]								
1	0.25	1.9	8.1	1	7.5	12.4	6	4.4	16.8	8
2	0.25	1.9	8.1	1	7.5	12.4	6	4.4	16.8	8
3	0.25	1.9	8.1	0	7.5	12.4	0	4.4	16.8	0
4	0.25	0	0	0	0	0	0	0	0	0
5	0.5	0	0	0	0	0	0	0	0	0

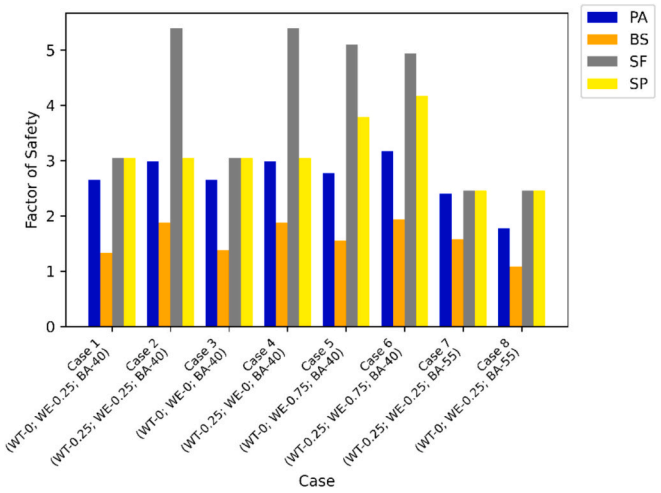

Fig. 12. Variation of FS for different bank configuration cases with additional root reinforcement in presence of PA (*Phragmites australis* L.), SF (*Salix fragilis* L.), SP(*Salix purpurea* L.) and BS (Bare soil) corresponding to input values of G1. Each group of four bars represents a case with varying Water Table (WT), Water flow Elevation (WE), and Bank Angle (BA) conditions.

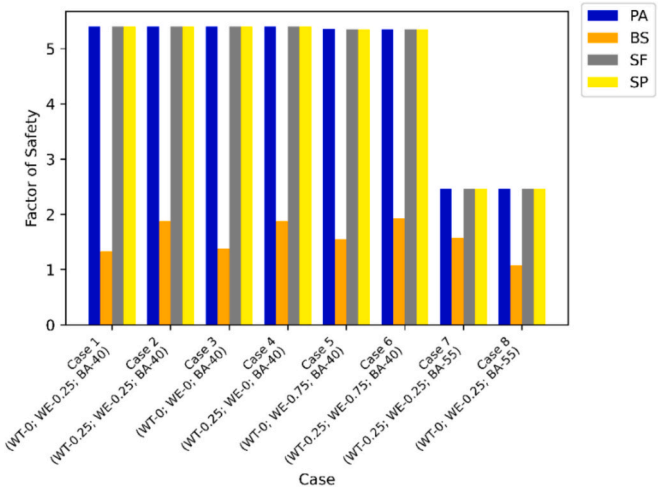

Fig. 13. Variation of FS for different bank configuration cases with additional root reinforcement in presence of PA (*Phragmites australis* L.), SF (*Salix fragilis* L.), SP(*Salix purpurea* L.) and BS (Bare soil) corresponding to input values of G2. Each group of four bars represents a case with varying Water Table (WT), Water flow Elevation (WE), and Bank Angle (BA) conditions.

composite only when it intersects the shear surface. However, even when a root is embedded within the corkscrew sample, it is included in the biomass measurements. Therefore, any comparison of root contribution to strength based on root biomass requires careful consideration of which roots to include in the biomass measurements. A similar challenge exists in direct shear tests: the biomass of roots that intersect the shear surface should be used for analysis, rather than the total root biomass in the sample. Consequently, only RAR was measured in tests on SP and CL.

Widely used root reinforcement prediction models, such as the Wu model Wu (1976) and the Fiber Bundle Model Pollen and Simon (2005), are based on root biomechanical properties (tensile strength, Young's modulus, etc.) and root quantity (RAR). The current study did not examine the tensile strength or root pullout characteristics of the three species, as the primary aim was direct measurement of root reinforcement. Additionally, it is important to note that the mechanical properties of roots from the same species can vary based on their location and

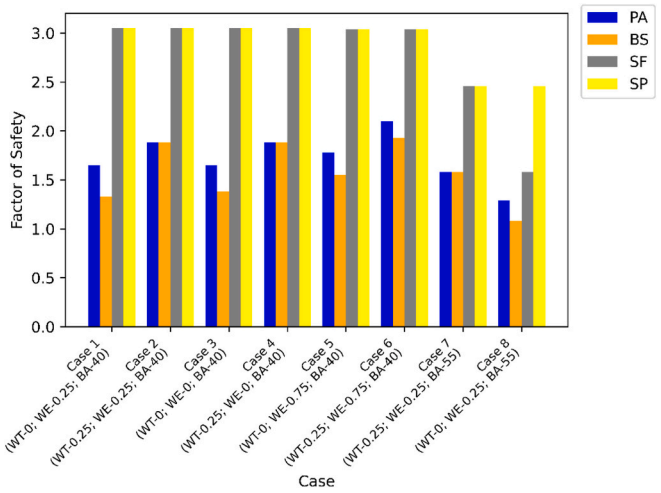

Fig. 14. Variation of FS for different bank configuration cases with additional root reinforcement in presence of PA (*Phragmites australis* L.), SF (*Salix fragilis* L.), SP(*Salix purpurea* L.) and BS (Bare soil) corresponding to input values of G3. Each group of four bars represents a case with varying Water Table (WT), Water flow Elevation (WE), and Bank Angle (BA) conditions.

the various growth stresses and moisture conditions they have experienced. Consequently, only a direct comparison between RAR and normalized peak strength and normalized energy was performed. The positive correlation between RAR and peak strength observed for SF and CL implies an increase in the mechanical properties of root-reinforced soils with increasing root quantity. Docker and Hubble (2008) observed a linear relationship between RAR and the increase in shear failure stress. A strong positive correlation between RAR and shear strength increase in planted soils was reported by Mickovski et al. (2009).

Normalized peak force and energy are not solely determined by root area ratio but are influenced by additional factors such as root biomechanical properties and soil-root interactions. The focus on linear regression with root area ratio as the primary variable, while simplifying the analysis, contributes to the observed variability and low R^2 values in some cases. The plots in Fig. 11 illustrate the general variation of root-soil composite strength in relation to root area ratio. The outliers (R^2 = 0.01 and 0.02) likely result from cases where root area ratio alone fails to capture the complexity of root-soil strength. For example, in scenarios with significant variations in root tensile strength, the relationship between root area ratio and strength becomes less linear. Conversely, the moderate R^2 values (0.62–0.65) may correspond to systems where root area ratio is a more dominant factor in determining peak strength, though these values still suggest room for improvement. This also indicates that the relationships may be species-dependent.

In the case of CL, despite the low recorded RAR values, the peak strength remained high. This discrepancy is most likely attributed to the comparatively higher tensile strengths of these roots, as observed by Docker and Hubble (2008).

4.2. Properties of root reinforced soils

Corkscrew extraction samples with higher RAR showed increased root-soil composite ductility for SF and SP (Fig. 15). This is similar to observations from in situ direct shear tests, where vegetated samples withstand greater shear displacements (Ekanayake and Phillips, 1999). Docker and Hubble (2008) also reported that tree roots provided their greatest contribution to soil strength at displacements where the soil alone would only provide residual strength. The abrupt declines in force-displacement graphs, often accompanied by an audible clicking sound observed in the current study, were similarly documented in direct shear

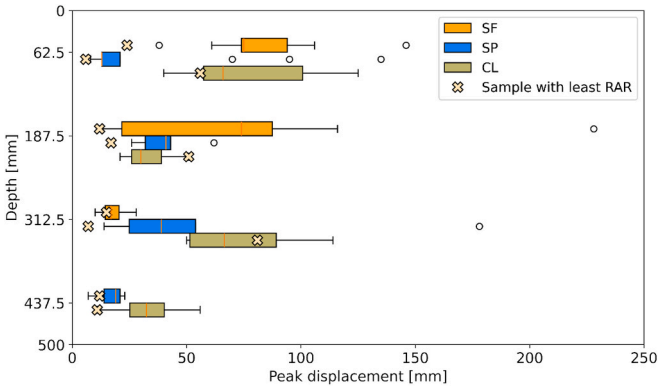

Fig. 15. Boxplots illustrating displacement at peak force measured from corkscrew extraction experiments at different depths (mm) for three species: *Salix fragilis* (SF), *Salix purpurea* (SP), and *Crataegus laevigata* (CL). The 'Sample with least RAR' represents the sample with the lowest Root Area Ratio within each depth interval. The boxes depict the interquartile range (IQR), with the median value indicated by a line within the box. Whiskers extend to 1.5 times the IQR, and outliers are plotted individually.

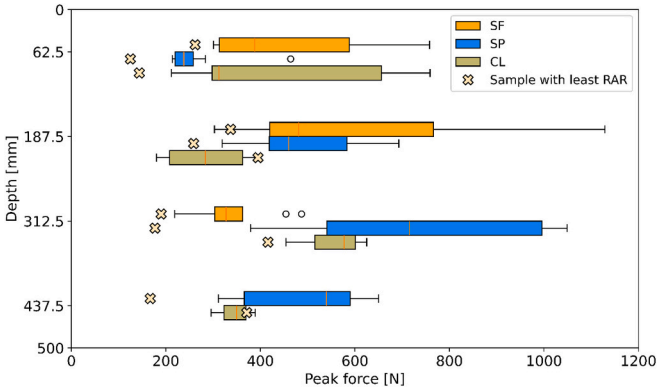

Fig. 16. Boxplots illustrating the peak force (N) measured from corkscrew extraction experiments at different depths (mm) for three species: *Salix fragilis* (SF), *Salix purpurea* (SP), and *Crataegus laevigata* (CL). The 'Sample with least RAR' represents the sample with the lowest Root Area Ratio within each depth interval. The boxes depict the interquartile range (IQR), with the median value indicated by a line within the box. Whiskers extend to 1.5 times the IQR, and outliers are plotted individually.

tests conducted by Docker and Hubble (2008) on four distinct riparian vegetation types. Meijer et al. (2018) also reported these phenomena in their study involving blackcurrant (*Ribes nigrum*) shrubs and Sitka spruce (*Picea sitchensis*) trees.

However, this ductility of rooted soil was not clearly observable in CL-rooted soil at all depths. In the majority of tests, the predominant failure mode observed was root breakage. Nevertheless, in CL sample extractions at depths of 125–250 mm and 375–500 mm, instances of root slippage were noted. In these particular tests, the root area ratio was notably greater compared to the other tests, even though the peak force was not. This finding aligns with previous studies (Schwarz et al., 2010; Ghestem et al., 2014), which proposed that roots exhibiting breakage rather than slippage tend to exhibit higher resistance, as they fully utilize their tensile strength. Whether root breakage or pullout occurs depends on a number of factors related to both soil (soil moisture, type, etc.) and vegetation (branching, size, etc.).

Species-dependent variation in force-displacement behavior was reported by Ghestem et al. (2014). However, no clear difference in force-displacement behavior among the three species was identified in this study. It should also be noted that insufficient shear strain displacement may have been achieved in direct shear tests to cause all roots to fail, whereas in this study, corkscrew extraction continued until all roots had been pulled out or ruptured. In general, SF and CL showed higher peak force in the top layers. In deeper layers (250–375 mm), SP-rooted soil showed higher resistance to shear (see Fig. 16).

Another aspect to consider, in addition to the additional strength provided to the slope, is the vegetation's self-weight, which negatively influences slope stability. For instance, CL can provide similar strength to SP in superficial layers with significantly less additional self-weight. However, this aspect is often excluded from root reinforcement studies and warrants further investigation. From a practical standpoint, the findings of Capobianco et al. (2021) suggest that implementing a mixed vegetation strategy, including trees, shrubs, and grasses, is the most effective way to achieve strong hydro-mechanical reinforcement of streambanks, alongside improved erosion protection and enhanced ecosystem biodiversity.

4.3. BSTEM modelling

Including the obtained corkscrew experimental results in the BSTEM model presents several challenges. Firstly, only peak shear strength is obtained from these experiments; soil parameters such as cohesion and internal friction angle are not directly available. Meijer et al. (2016) found that corkscrew experiments and direct shear tests show similar peak strengths in bare soil. Nevertheless, it should be noted that corkscrew tests are conducted under very low normal stress (<10 kPa). Secondly, corkscrew experiments have a vertical shear plane, whereas the bank failure plane is expected to be horizontal (Meijer et al., 2016). Lastly, BSTEM accounts for root reinforcement by adding the additional cohesion due to the presence of vegetation to the top 1 m of the bank. Furthermore, the model does not account for cases where vegetation cover extends over the entire bank slope (Krzeminska et al., 2019). Nevertheless, the current study attempted to address the above drawbacks by using three different groups of input values for each species to represent the increase in strength due to the presence of roots.

The FS for all vegetated cases was higher than for corresponding bare soil cases, as observed in other field investigations (e.g., Zong et al., 2023). It can also be observed that the presence of vegetation reinforcement compensates for the increase in bank angle to 55°. When the bank angle increases to 55°, a 1.9 kPa and 1 kPa increase in cohesion due to the roots of PA would result in a FS of 1.78 (stable) and 1.29 (conditionally stable), respectively. However, in the absence of vegetation, the same bank would be unstable, with a FS of 1.08.

Although an increase in root reinforcement results in an increase in the FS, there appears to be a critical cohesion value beyond which further increases have only a limited effect on the FS. This can be observed by comparing the FS for model results using corkscrew experiment results (G2). The increase in root reinforcement values from 8.1 kPa to 12.4 kPa to 16.8 kPa had no influence on the FS for any of the eight cases analyzed. Similar observations have also been made regarding the effect of root reinforcement on slope settlement during earthquake loading (Liang et al., 2020). This implies that vegetation management for nature-based solutions for bank protection (Gray and Sotir, 1996) should aim to achieve this critical cohesion value to maximize the benefits of root reinforcement.

4.4. Advantages and limitations of the corkscrew method for assessing root reinforcement

The corkscrew setup proved to have several advantages for monitoring root reinforcement along canal and stream banks. The relatively short time required to conduct the tests allows for larger-scale testing and application. Its ease of use and light weight enable testing even in challenging riparian conditions. Another clear advantage compared to field direct shear tests is the ability to conduct semi-destructive testing without significantly affecting the overall stability of the embankment.

This offers the possibility of using the method periodically to monitor root reinforcement along canal embankments.

The corkscrew extraction technique, while offering certain advantages, presents several limitations. The small sample volume of the corkscrew technique can lead to biased results if encountered roots are unusually large or dense Meijer et al. (2019). Furthermore, the variability in site characteristics can complicate the isolation and quantification of the specific contribution of root reinforcement to bank stability. Conducting tests very close to canals or water bodies can present logistical challenges, as a stable tripod setup may not always be feasible. Challenges can arise in achieving the desired testing depth. Manual insertion of the corkscrew can be physically demanding and may limit the maximum achievable depth (in this study, 500 mm). Moreover, accurately reinserting the corkscrew into the same hole after a previous test at a shallower depth can be challenging and may introduce variability into the measurements. The technique can also be less effective in soils with high gravel content or where roots exhibit primarily horizontal growth Meijer et al. (2019). In this study recovery of roots after the tests from the corkscrew hole was difficult, thus making the comparison with root mechanical properties challenging.

To mitigate these limitations, several strategies can be implemented. Following Meijer et al. (2019), increasing the number of samples per location can improve the statistical reliability of the measurements, allowing for a more accurate estimation of the mean root reinforcement strength. Modifying the corkscrew apparatus, such as by using longer handles and larger helixes, can potentially increase the achievable testing depth and reduce variability. Alternative setups, such as those utilizing specialized drilling equipment, may be necessary to overcome limitations in accessing deeper root systems. Adapting the setup to conduct the corkscrew extractions at an angle to the vertical can also be useful. To improve recovery of roots foam could be used after the tests as done by Meijer et al. (2018). However, the primary objective of this study was not to determine mechanical properties of roots, and hence, root recovery was done only manually. Furthermore, conducting calibration tests in a variety of soil types and with different vegetation species is crucial to develop correction factors and improve the generalizability of the method.

5. Conclusions

Corkscrew extraction experiments proved to be a quick and useful tool for determining the strength of root-reinforced soil along canal banks. With further development, the setup could serve as an effective monitoring tool for root reinforcement along canal and river embankments. Of the three species investigated in this study, soil rooted with *Salix fragilis* L. and *Crataegus laevigata* DC. showed higher resistance to shear in the top layer (0–250 mm), while *Salix purpurea* L. showed higher resistance in deeper layers (250–500 mm). Root breakages were identified by sudden drops in the force-displacement curve, often accompanied by an audible clicking sound. Overall, samples with higher root area ratios exhibited greater peak strength and higher displacement at peak force compared to those with the lowest root area ratios across all three species and depths, with the exception of *Crataegus laevigata* DC. at depths of 125–250 mm and 375–500 mm. The large number of in situ tests that can be conducted using corkscrew experiments proves useful where high variability is observed. Modelling using BSTEM indicates a minimum “critical” root reinforcement level beyond which the influence of root reinforcement on the factor of safety is minimal. Even moderate amounts of root reinforcement were seen to increase the FS of the bank. The presence of vegetation was able to counteract the effect of an increase in bank angle.

This study acknowledges several limitations. While providing initial insights, the analysis was based on a limited sample size. Seasonal variations in root reinforcement, a factor likely influencing long-term bank stability, were not measured or incorporated into the modelling. The confinement of the study to a limited soil type and plant per species also presents challenges for broad generalization and scalability of the findings. Future research should address these limitations by investigating these species across diverse locations and site conditions, considering variations in soil type, hydrology, and competition with other vegetation. Increasing the number of tests will be crucial to enhance the statistical power of the analysis and better account for inherent variability. Finally, incorporating the effect of vegetation self-weight into bank stability models like BSTEM will provide a more comprehensive understanding of the forces at play, particularly for larger vegetation. Addressing these aspects in future investigations will further refine our understanding of root reinforcement mechanics and contribute to the development of more robust and effective bioengineering strategies for slope stabilization.

CRediT authorship contribution statement

Abhijith Kamath: Writing – original draft, Project administration, Investigation, Funding acquisition, Conceptualization. **Karine van Bergen:** Writing – original draft, Investigation, Data curation. **Geert Ravenshorst:** Writing – review & editing, Supervision, Methodology. **Jan-willem van de Kuilen:** Writing – review & editing, Project administration, Methodology, Funding acquisition.

Declaration of competing interest

The authors declare that they have no known competing financial interests or personal relationships that could have appeared to influence the work reported in this paper.

Acknowledgements

The authors gratefully acknowledge the *Provincie Noord-Holland* for having funded the research study.

Appendix A. Supplementary data

Supplementary data to this article can be found online at https://doi.org/10.1016/j.ecoleng.2025.107623.

Data availability

Data will be made available on request.

References

Abernethy, B., Rutherfurd, I.D., 2001. The distribution and strength of riparian tree roots in relation to riverbank reinforcement. Hydrol. Process. 15 (1), 63–79.

Alam, M., Jiang, Y.J., Umar, M., Su, L. Jun, Rahman, M., Ullah, F., 2022. Influence of drainage and root biomass on soil mechanical behavior in triaxial tests. Acta Geotech. 17 (7). https://doi.org/10.1007/s11440-021-01380-w.

Bischetti, G.B., Chiaradia, E.A., Simonato, T., Speziali, B., Vitali, B., Vullo, P., Zocco, A., 2005. Root strength and root area ratio of forest species in lombardy (Northern Italy). Plant Soil 278 (1–2). https://doi.org/10.1007/s11104-005-0605-4.

Boldrin, D., Leung, A.K., Bengough, A.G., 2017. Root biomechanical properties during establishment of woody perennials. Ecol. Eng. 109. https://doi.org/10.1016/j.ecoleng.2017.05.002.

Capobianco, V., Robinson, K., Kalsnes, B., Ekeheien, C., Høydal, Ø., 2021. Hydro-mechanical effects of several riparian vegetation combinations on the streambank stability — a benchmark case in southeastern Norway. Sustainability (Switzerland) 13 (7). https://doi.org/10.3390/su13074046.

Docker, B.B., Hubble, T.C.T., 2008. Quantifying root-reinforcement of river bank soils by four Australian tree species. Geomorphology 100 (3–4), 401–418. https://doi.org/10.1016/j.geomorph.2008.01.009.

Ekanayake, J.C., Phillips, C.J., 1999. A method for stability analysis of vegetated hillslopes: an energy approach. Can. Geotech. J. 36 (6). https://doi.org/10.1139/t99-060.

Fan, C.C., Chen, Y.W., 2010. The effect of root architecture on the shearing resistance of root-permeated soils. Ecol. Eng. 36 (6), 813–826. https://doi.org/10.1016/j.ecoleng.2010.03.003.

Fan, C.C., Su, C.F., 2008. Role of roots in the shear strength of root-reinforced soils with high moisture content. Ecol. Eng. 33 (2). https://doi.org/10.1016/j.ecoleng.2008.02.013.

Fan, C.C., Tsai, M.H., 2016. Spatial distribution of plant root forces in root-permeated soils subject to shear. Soil Tillage Res. 156. https://doi.org/10.1016/j.still.2015.09.016.

Ghestem, M., Veylon, G., Bernard, A., Vanel, Q., Stokes, A., 2014. Influence of plant root system morphology and architectural traits on soil shear resistance. Plant Soil 377 (1–2), 43–61. https://doi.org/10.1007/s11104-012-1572-1.

Giadrossich, F., Schwarz, M., Cohen, D., Cislaghi, A., Vergani, C., Hubble, T., Phillips, C., Stokes, A., 2017. Methods to measure the mechanical behaviour of tree roots: a review. Ecol. Eng. 109. https://doi.org/10.1016/j.ecoleng.2017.08.032.

Gray, D.H., Sotir, R.B., 1996. Biotechnical and Soil Bioengineering Slope Stabilization: A Practical Guide for erosion Control. John Wiley & Sons.

Kamath, A., van Bergen, K., Ravenshorst, G., van de Kuilen, J.W., 2023, December. Applicability of corkscrew extraction technique in strength characterization of *Phragmites australis* rooted soil. In: International Conference on Geotechnics for Sustainable Infrastructure Development. Springer Nature Singapore, Singapore, pp. 1789–1800.

Klavon, K., Fox, G., Guertault, L., Langendoen, E., Enlow, H., Miller, R., Khanal, A., 2017. Evaluating a process-based model for use in streambank stabilization: insights on the Bank Stability and Toe Erosion Model (BSTEM). Earth Surf. Process. Landf. 42 (1). https://doi.org/10.1002/esp.4073.

Krzeminska, D., Kerkhof, T., Skaalsveen, K., Stolte, J., 2019. Effect of riparian vegetation on stream bank stability in small agricultural catchments. Catena 172. https://doi.org/10.1016/j.catena.2018.08.014.

LeRoy, J.Z., Heimann, D.C., Hix, K.D., Cigrand, C.V., Burk, T.J., 2024. Geomorphic Change, Hydrology, and Hydraulics of Caulks Creek, Wildwood, Missouri (U.S. Geological Survey Scientific Investigations Report 2024–5079). U.S. Geological Survey. https://doi.org/10.3133/sir20245079.

Liang, T., Knappett, J.A., Leung, A.K., Glyn Bengough, A., 2020. Modelling the seismic performance of root-reinforced slopes using the finite-element method. Geotechnique 70 (5). https://doi.org/10.1680/jgeot.17.P.128.

Lohnes, R.A., Handy, R.L., 1968. Slope angles in friable loess. J. Geol. 76 (3). https://doi.org/10.1086/627327.

Meijer, G.J., Bengough, A.G., Knappett, J.A., Loades, K.W., Nicoll, B.C., 2016. New in situ techniques for measuring the properties of root-reinforced soil – laboratory evaluation. Geotechnique 66. https://doi.org/10.1680/jgeot.15.P.060.

Meijer, G.J., Bengough, A.G., Knappett, J.A., Loades, K.W., Nicoll, B.C., 2018. In situ measurement of root reinforcement using corkscrew extraction method. Can. Geotech. J. 55 (10). https://doi.org/10.1139/cgj-2017-0344.

Meijer, G., Bengough, G., Knappett, J., Loades, K., Nicoll, B., 2019. Measuring the strength of root-reinforced soil on steep natural slopes using the corkscrew extraction method. Forests 10 (12). https://doi.org/10.3390/F10121135.

Mickovski, S.B., Hallett, P.D., Bransby, M.F., Davies, M.C.R., Sonnenberg, R., Bengough, A.G., 2009. Mechanical reinforcement of soil by willow roots: impacts of root properties and root failure mechanism. Soil Sci. Soc. Am. J. 73 (4), 1276–1285. https://doi.org/10.2136/sssaj2008.0172.

Midgley, T.L., Fox, G.A., Heeren, D.M., 2012. Evaluation of the bank stability and toe erosion model (BSTEM) for predicting lateral retreat on composite streambanks. Geomorphology 145–146. https://doi.org/10.1016/j.geomorph.2011.12.044.

Pollen, N., 2007. Temporal and spatial variability in root reinforcement of streambanks: Accounting for soil shear strength and moisture. Catena 69 (3). https://doi.org/10.1016/j.catena.2006.05.004.

Pollen, N., Simon, A., 2005. Estimating the mechanical effects of riparian vegetation on stream bank stability using a fiber bundle model. Water Resour. Res. 41 (7), 1–11. https://doi.org/10.1029/2004WR003801.

Pollen-Bankhead, N., Simon, A., 2009. Enhanced application of root-reinforcement algorithms for bank-stability modeling. Earth Surf. Process. Landf. 34 (4). https://doi.org/10.1002/esp.1690.

Rasouli, M.O., Sadat, S.H., Xenarios, S., 2020. Evaluating stream bank instability and toe erosion using BSTEM model for the Amu river. J. Environ. Sci. Revolut. 1 (1). https://doi.org/10.37357/1068/jesr/1.1.01.

Schwarz, M., Cohen, D., Or, D., 2010. Root-soil mechanical interactions during pullout and failure of root bundles. J. Geophys. Res. F Earth Surf. 115 (4), 1–19. https://doi.org/10.1029/2009JF001603.

Simon, A., Curini, A., Darby, S.E., Langendoen, E.J., 2000. Bank and near-bank processes in an incised channel. Geomorphology 35 (3–4). https://doi.org/10.1016/S0169-555X(00)00036-2.

Simon, A., Pollen-Bankhead, N., Mahacek, V., Langendoen, E., 2009. Quantifying reductions of mass-failure frequency and sediment loadings from streambanks using toe protection and other means: Lake Tahoe, United States. J. Am. Water Resour. Assoc. 45 (1). https://doi.org/10.1111/j.1752-1688.2008.00268.x.

Simon, A., Pollen-Bankhead, N., Thomas, R.E., 2011. Development and application of a deterministic bank stability and toe erosion model for stream restoration. Geophys. Monogr. Ser. 194. https://doi.org/10.1029/2010GM001006.

Symmank, L., Natho, S., Scholz, M., Schröder, U., Raupach, K., Schulz-Zunkel, C., 2020. The impact of bioengineering techniques for riverbank protection on ecosystem services of riparian zones. Ecol. Eng. 158. https://doi.org/10.1016/j.ecoleng.2020.106040.

Tardío, G., Mickovski, S.B., 2016. Implementation of eco-engineering design into existing slope stability design practices. Ecol. Eng. 92. https://doi.org/10.1016/j.ecoleng.2016.03.036.

Tardio, G., Mickovski, S.B., 2023. A novel integrated design methodology for nature-based solutions and soil and water bioengineering interventions: the Tardio&Mickovski methodology. Sustainability (Switzerland) 15 (4). https://doi.org/10.3390/su15043044.

Ursic, M.E., Langendoen, E.J., 2021. Bank Stability and Toe Erosion (BSTEM) – User's Manual (Research Report No. 82).. USDA Agricultural Research Service National Sedimentation Laboratory.

Wu, T.H., 1976. Investigation of Landslides on Prince of Wales Island. Ohio State University, Alaska.

Yildiz, A., Graf, F., Rickli, C., Springman, S.M., 2018. Determination of the shearing behaviour of root-permeated soils with a large-scale direct shear apparatus. Catena 166 (February 2017), 98–113. https://doi.org/10.1016/j.catena.2018.03.022.

Zhang, C.B., Chen, L.H., Liu, Y.P., Ji, X.D., Liu, X.P., 2010. Triaxial compression test of soil-root composites to evaluate influence of roots on soil shear strength. Ecol. Eng. 36 (1), 19–26. https://doi.org/10.1016/j.ecoleng.2009.09.005.

Zong, Q., Zheng, T., Tang, R., Jin, K., Li, L., Qin, P., Liu, C., 2023. Effects of desert riparian vegetation roots on the riverbank retreat process in the Tarim River in China. J. Hydrol. 617. https://doi.org/10.1016/j.jhydrol.2022.128894.